Visual Neuroscience (1995), **12**, 723-741. Printed in the USA.

Receiver operating characteristic (ROC) analysis of neurons in the cat's lateral geniculate nucleus during tonic and burst response mode

W. GUIDO, S.-M. LU, J. W. VAUGHAN, DWAYNE W. GODWIN, AND S. MURRAY SHERMAN

Department of Neurobiology, State University of New York, Stony Brook

(RECEIVED August 9, 1994; ACCEPTED January 9, 1995)

Abstract

Relay cells of the lateral geniculate nucleus respond to visual stimuli in one of two modes: *burst* and *tonic*. The burst mode depends on the activation of a voltage-dependent, Ca^{2+} conductance underlying the *low threshold spike*. This conductance is inactivated at depolarized membrane potentials, but when activated from hyperpolarized levels, it leads to a large, triangular, nearly all-or-none depolarization. Typically, riding its crest is a high-frequency barrage of action potentials. Low threshold spikes thus provide a nonlinear amplification allowing hyperpolarized relay neurons to respond to depolarizing inputs, including retinal EPSPs. In contrast, the tonic mode is characterized by a steady stream of unitary action potentials that more linearly reflects the visual stimulus. In this study, we tested possible differences in detection between response modes of 103 geniculate neurons by constructing *receiver operating characteristic* (ROC) curves for responses to visual stimuli (drifting sine-wave gratings and flashing spots). Detectability was determined from the ROC curves by computing the area under each curve, known as the *ROC area*. Most cells switched between modes during recording, evidently due to small shifts in membrane potential that affected the activation state of the low threshold spike. We found that the more often a cell responded in burst mode, the larger its ROC area. This was true for responses to optimal and nonoptimal visual stimuli, the latter including nonoptimal spatial frequencies and low stimulus contrasts. The larger ROC areas associated with burst mode were due to a reduced spontaneous activity and roughly equivalent level of visually evoked response when compared to tonic mode. We performed a within-cell analysis on a subset of 22 cells that switched modes during recording. Every cell, whether tested with a low contrast or high contrast visual stimulus exhibited a larger *ROC area* during its burst response mode than during its tonic mode. We conclude that burst responses better support signal detection than do tonic responses. Thus, burst responses, while less linear and perhaps less useful in providing a detailed analysis of visual stimuli, improve target detection. The tonic mode, with its more linear response, seems better suited for signal analysis rather than signal detection.

Keywords: Visual system, Low threshold Ca^{2+} conductance, Signal detection, Thalamus

Introduction

Relay cells of the cat's lateral geniculate nucleus (LGN) respond to a visual stimulus in one of two modes, *tonic mode* or *burst mode** (Guido et al., 1992; Lu et al., 1992). These modes depend on the relay cell's resting membrane potential (Lo et al., 1991; Lu et al., 1992, 1993), because they are based on the activation state of a voltage-dependent Ca^{2+} conductance that underlies the low threshold spike (e.g. Jahnsen & Llinás, 1984*a*,*b*; Deschênes et al., 1984; Crunelli et al., 1989). It is *inactivated* by membrane depolarization more positive than about −60 mV, but it is *de-inactivated* at more hyperpolarized levels from which it can be *activated* by a suitably large depolarization, such as an EPSP. It leads to a largely all-or-none, spike-like depolarization due to Ca^{2+} entry. Because this depolarizing spike is activated at a relatively hyperpolarized membrane level lower than that required for activating a conventional action potential, it is called *low threshold*. A high-frequency burst of conventional action potentials occurs at the peak of the low threshold spike. Occasionally, following each burst are a few conventional action potentials; more typically, between low thresholds spikes and the concomitant bursts of action potentials, the cell is relatively silent. This pattern of bursts separated by fairly silent

Reprint requests to: S.M. Sherman, Department of Neurobiology, State University of New York, Stony Brook, NY 11794-5230, USA.

Present address of W. Guido: LSU Medical Center, Dept. of Anatomy and Center for Neuroscience, 1901 Perdido Street, New Orleans, LA 70112, USA.

Present address of S.-M. Lu: Institute for Developmental Neuroscience, Kennedy Center, Box 152 Peabody College, Vanderbilt University, Nashville, TN 37203, USA.

**Tonic* used in this sense refers to a response mode of a geniculate relay cell, and here it is paired with *burst*. Both X and Y cells display both response modes. This should not be confused with another use of *tonic* when paired with *phasic* to refer to a cell type: *tonic* for X and *phasic* for Y. Throughout this paper, we shall use *tonic* only to refer to response mode and not to cell type.

periods typifies the burst mode of firing. The low threshold spike provides an amplification that expedites the generation of action potentials in a hyperpolarized cell. However, because of the largely all-or-none, spike-like depolarization of the low threshold spike, the amplification is nonlinear (Guido et al., 1992; Lu et al., 1992, 1993). At depolarized levels during which the low threshold spike is inactivated (i.e. during tonic mode firing), the cell responds with a steady stream of action potentials with a frequency and duration that corresponds fairly linearly to stimulus strength and duration.

This suggests that the tonic mode, with its more faithful linear summation in response to visual targets, is better suited to convey detailed information about visual stimuli. For what function, then, might the burst mode be better suited? One possibility suggested by the difference between the tonic and burst response patterns is that burst firing supports better signal detection. This is because burst firing is characterized by a fairly robust response, albeit nonlinear, and the relative silence between bursts suggests little spontaneous activity. Thus, burst firing might be associated with an elevated ratio of signal (i.e. visual response) to noise (i.e. spontaneous activity).

The main purpose of this study, therefore, was to test formally whether geniculate neurons exhibit different levels of signal detectability during tonic and burst firing. A powerful means of measuring such detectability is to construct *receiver operating characteristic* (ROC) curves (Green & Swets, 1966; Macmillan & Creelman, 1991) for neuronal responses (Cohn et al., 1975; Tolhurst et al., 1983; Wilson et al., 1988; Holdefer et al., 1989; Britten et al., 1992). ROC curves offer an unbiased means to distinguish visually driven from spontaneous activity, because they do not depend on a fixed criterion to determine whether a threshold response has been reached.

Methods

We performed experiments on adult cats (1.8–3.0 kg) using methods that have been described in detail elsewhere (Bloomfield et al., 1987; Bloomfield & Sherman, 1988; Lo et al., 1991; Lu et al. 1992) and which are only briefly outlined here.

Animal preparation and recording

For initial surgical preparation, we anesthetized the cats with 2–3% halothane in N_2O/O_2 mixed in a 1:1 ratio. We maintained anesthesia throughout the recording session with 0.3–1.0% halothane in a 7:3 mixture of N_2O/O_2. For paralysis, we administered 4.0 mg of gallamine triethiodide followed by a mixture of 3.6 mg/h of gallamine triethiodide and 0.7 mg/h of d-tubocurarine in 5% lactated Ringer's solution. Cats were artificially respired through a tracheal cannula. We treated all wound edges and pressure points with a long-lasting topical anesthetic. Rectal temperature, heart rate, and end-tidal CO_2 were monitored and kept within normal physiological limits. We also monitored electroencephalogram (EEG) during the anesthesia and paralysis, the typically synchronous EEG activity was occasionally interrupted by brief episodes of spindle activity (Ikeda & Wright, 1975; Funke & Eysel, 1992). However, because we did not store EEG data, no attempt could be made to correlate EEG activity with response mode of geniculate neurons.

We mounted the cat in a stereotaxic apparatus and opened the skull above the lateral geniculate nucleus (centered on A 5.0, L 9.0) to permit passage of the recording electrode. A plastic well was built around the craniotomy, and the chamber sealed with agar and wax to improve stability during recording. We made another, smaller craniotomy along the midline above the optic chiasm (centered on A 13.0 and extending 2.0 mm to each side of the midline) and inserted a pair of bipolar stimulating electrodes through this to straddle the optic chiasm. We applied single pulses (0.1-ms duration, 100–500 μA, <1 Hz) across these electrodes to activate geniculate neurons orthodromically from the optic tract.

The pupils were dilated, accommodation was blocked pharmacologically, and the corneas were protected with zero-power contact lenses that contained an artificial pupil with a diameter of 3 mm. We used a fiber optic light source to plot and project retinal landmarks, including the optic disk and *area centralis*, onto a frontal tangent screen positioned 57.0 cm from the nodal points of the eyes. We used streak retinoscopy to choose appropriate spectacle lenses for focusing the eyes onto the same tangent screen or onto an electronic display monitor placed in front of the cat. The display monitor was placed 28.5 cm in front of the eyes.

Single neurons in the geniculate A-laminae were recorded intracellularly and extracellularly using fine-tipped micropipettes filled with 2–4 M KAc or 2 M NaCl (extracellular only). The electrode impedances ranged from 20 to 40 MΩ. Requirements for acceptable intracellular recording are explained elsewhere (Bloomfield et al., 1987; Lo et al., 1991; Lu et al., 1992). Neuronal activity was amplified through a high-impedance amplifier, displayed on an oscilloscope, fed through an audio monitor, and stored on an 8-channel FM tape recorder interfaced with a computer for off-line analysis. We fed action potentials through a window discriminator for off-line computer analysis. We stored the spike arrival times of the responses to visual stimuli with a resolution of 0.1 ms.

Visual stimulation and cell classification

For initial evaluation of receptive-field properties, we flashed small spots of light on the tangent screen using a hand-held projector. We thereby determined ocular dominance, receptive-field location, receptive-field size, and center type. We then replaced the tangent screen with a display monitor to present either vertically oriented sine-wave gratings or square-wave modulated, bright and dark spots on a moderate background.

Grating stimulation

We maintained the gratings at a space average luminance of 30 cd/m^2 and used a range of contrasts, spatial frequencies, and temporal frequencies; we also could either drift or counterphase modulate them. Typically, we drifted the gratings at a contrast of 0.5 and at spatiotemporal parameters that evoked the maximum response. To obtain a measure of spontaneous activity, we reduced grating contrast to 0, resulting in a diffuse field with a luminance of 30 cd/m^2. For some neurons, we constructed complete spatial tuning or contrast vs. response functions at a temporal frequency of 4 Hz. Responses were evaluated by computing the Fourier components from averaged histograms. These histograms for each set of parameters were based on $\geq$50 s of stimulation, the number of cycles dependent on temporal frequency (e.g. $\geq$200 trials at 4 Hz). To minimize uncontrolled response variables with grating stimuli, we interleaved trials of visual activity with those of spontaneous activity.

Spot stimulation

For many neurons, we also presented dark and bright spots of light the diameter of, and centered on, the receptive-field center. Two different paradigms were used to stimulate the cells, and we averaged the responses to 50–100 or more trials. In the first, we used simple square-wave modulation at 0.5–1.0 Hz between background (30 cd/m^2, i.e. the same average luminance as the gratings) and either a dark spot (10–22 cd/m^2) for off-center cells or a bright spot (45–90 cd/m^2) for on-center cells. In the second, we used a five-part sequence, each of 500-ms duration: (1) background (30 cd/m^2) with no spot, (2) dark spot (10 cd/m^2 against the background of 30 cd/m^2), (3) background with no spot, (4) bright spot (90 cd/m^2 against the background of 30 cd/m^2), and (5) background with no spot. As with the gratings, spontaneous activity was based on responsiveness during presentation of the background only (see below). Since each stimulus trial contained both spontaneous and visually driven activity, interleaving of these epochs was unnecessary.

Response classification

We classified all geniculate neurons as X or Y using a standard battery of tests. This included linearity of spatial summation in response to grating stimuli, receptive-field center size, response latency to electrical stimulation of optic chiasm, and response to a large, fast moving stimulus of high contrast to activate the surround (i.e. dark for an on-center cell and *vice versa*). We used our previously described criteria (Guido et al., 1992; Lu et al., 1992, 1993) to distinguish between tonic and burst response modes for these cells. Briefly, a response is considered to be due to a low threshold burst if its component action potentials exhibit interspike intervals $\leq$4 ms and if the first spike in the burst epoch occurs after a silent period $\geq$100 ms. To describe the overall tendency of a cell to respond in tonic or burst mode, we determined a *burst index* for each, which is simply the percentage of trials (whether a cycle of the drifting grating or of the spot stimulation) to which the cell responded to the visual stimulus in burst mode (for details of the burst index, see Guido et al., 1992).

ROC analysis

ROC curves (for details of ROC methodology, see Green & Swets, 1966; Pollack & Hsieh, 1969; Cohn et al., 1975; Macmillan & Creelman, 1991) were derived from probability distributions of spike density counts obtained during a sampling episode (τ) of visually driven (τ_s) and spontaneous activity (τ_n). We determined the probability that a neuron fired a criterion number of spikes for τ_s and τ_n, using the following procedure based on samples of 50–100 trials each of visually driven (i.e. cycles of stimulation) and spontaneous activity. For each cell, we set a criterion domain which corresponded to the full range of spikes occurring for τ_s and τ_n. For the resultant ROC curve, we simply plot for all criterion levels P (*false alarm*) on the abscissa *vs.* P (*hit*) on the ordinate: P (*hit*) is the probability of attaining a criterion response during τ_s, and P (*false alarm*) is the probability of attaining a criterion response during τ_n. Each ROC curve is plotted against a line of unity slope, the line representing the locus of points of equal probabilities for τ_s and τ_n. To analyze ROC curves, we used a method which involves computing the area under the ROC curve (Green & Swets, 1966; Macmillan & Creelman, 1991). Area under the ROC curve (which we hereafter refer to as ROC area) provides a distribution-free estimate of proportion correct for an ideal observer in a two-alternative forced-choice procedure. Thus, ROC area becomes a nonparametric measure of discrimination performance (Green & Swets, 1966; see Pollack & Hsieh, 1969; Macmillan & Creelman, 1991). The area under the ROC curve can vary between 0 and 1.0, and an area of 0.5 is taken as representing signal detection no better than noise (e.g. the area represented by the line of unity slope). Thus, in practice, ROC areas representing actual signal detection vary between 0.5 and 1.0. There is a monotonic but nonlinear relationship between ROC area and signal detectability (Green & Swets, 1966; Pollack & Hsieh, 1969; Macmillan & Creelman, 1991).

Grating stimulation

For responses to gratings, τ_s was equal to half of the temporal period of the drifting grating and was centered on the positive phase (i.e. excitatory or on response) of the fundamental Fourier response component (F1). Thus for each cell, the location of τ_s shifted with respect to stimulus onset and depended entirely on the location of the positive phase of the fundamental response. Activity associated with the other half of the temporal period (i.e. inhibitory or off response) was not included in τ_s. We sampled activity for an equivalent period during presentation of the diffuse field for τ_n. With few exceptions, gratings were drifted at 4 Hz and thus τ_s and τ_n were each 125 ms.

Spot stimulation

The sampling episodes for spot stimulation differed somewhat depending on whether we used simple square-wave modulation or the more complex five-part stimulus cycle (see above for details). We found no detectable difference in any of our response measures between the two types of spot stimulation; while the differences for sampling episodes are explained in the following, for the remainder of this paper, we shall simply refer to both as spot stimulation. For simple square-wave stimulation, the period for τ_n was the final 250 ms of background activity, before the dark or bright spot came on; τ_s began with spot onset and lasted for 250 ms. For the five-part stimulation (see above for details), τ_n was the first 250 ms of the first (background) period, and τ_s was the first 250 ms of either the second (dark spot) period for off-center cells or the fourth (bright spot) period for on-center cells.

Statistics

Nonparametric statistics were used throughout. For comparison of mean values between cell populations, we used the Mann-Whitney U test. For within cell comparisons, we used the binomial test. For correlations, we used the Spearman rank correlation coefficient, r_s.

Results

We recorded activity from a total of 103 geniculate neurons: 90 extracellularly (33 X and 57 Y), and 13 intracellularly (six X, seven Y). The intracellularly recorded cells were visually stimulated with gratings. Of the 90 recorded extracellularly, 59 were tested with gratings, 42 with flashing spots, and 11 were tested with both types of stimuli. All of the 39 X cells and 54 of the 64 Y cells were located in the A-laminae, while the remaining ten Y cells were recorded in the magnocellular C-laminae.

Effect of response mode on spontaneous activity

Two factors that strongly influence a cell's ability to detect visual targets are the magnitude of visually driven activity (signal) and the degree of background or spontaneous activity (noise). Our previous studies have shown that, in hyperpolarized cells, visually evoked EPSPs can reliably trigger low threshold Ca^{2+} spikes leading to burst responses (Lo et al., 1991; Guido et al., 1992; Lu et al., 1992, 1993). The amplitude of these responses can be surprisingly high due to the nonlinear amplification afforded by the depolarizing low threshold spike, which is largely all-or-none in nature. What is not clear is what level of spontaneous activity is associated with burst responses. On the one hand, it might be quite low due to the associated hyperpolarization and/or the silent period between bursts (see Introduction and below). On the other hand, if its underlying EPSPs are sufficiently large to activate low threshold Ca^{2+} spikes, it might be relatively high, because even with the silent period (see Methods), the number of action potentials in the burst (≤ 10) can lead to spontaneous rates approaching 100 spikes/s.

To determine this, we examined the relationship between a cell's mode of firing during visual stimulation and its level of spontaneous activity for the 90 geniculate cells recorded extracellularly. Estimates of spontaneous activity were based on responses to a diffuse field (or zero-contrast uniform field) with an average luminance of 30 cd/m^2, and response mode (tonic *vs.* burst) was determined by the pattern of firing (see Methods; see also Guido et al., 1992; Lu et al., 1992). We regarded all other activity as tonic firing. In practice, we found that most cells displayed burst responses to many, but not all, trials of visual stimulation and that this burst response with few exceptions was the only response seen to a visual stimulus (see also Guido et al., 1992). The observation that cells typically responded to some trials in tonic mode and to others in burst mode was apparently due to minor fluctuations in membrane potential between trials that can inactivate or de-inactivate the low threshold Ca^{2+} conductance underlying burst responses (Lo et al., 1991; Lu et al., 1993). This intertrial variability is considered further below. To describe the overall tendency of a cell to respond in tonic or burst mode, we determined a burst index for each cell (see Methods). Of the 90 cells studied extracellularly, 13 (four X and nine Y) had a burst index of 0, and all of the rest had a burst index between 0 and 1, the highest being 0.98.

Fig. 1 shows the relationship between spontaneous activity and burst index. These variables are significantly and negatively correlated (for all cells, $r_s = -0.64$; $P < 0.001$; for X cells, $r_s = -0.65$, $P < 0.001$; and for Y cells, $r_s = -0.62$, $P < 0.001$). We thus conclude that, as a cell responds to visual stimuli more often in the burst mode, its spontaneous activity declines.

Since the burst mode is associated with a hyperpolarized membrane potential and silent periods between bursts, it may seem unsurprising at first glance that this results in reduced spontaneous activity. However, if this relationship between burst mode and responsiveness were so simple, this mode should also be associated with a comparable reduction in responses to visual stimulation. That is, both noise (spontaneous activity) and signal (response to visual targets) should be comparably reduced, and there should be no consistent or obvious effect of the burst response on signal detection. As we show below, this is not the case, since visual responses during burst mode are not appreciably reduced, and we thus emphasize that the reduced spontaneous activity associated with this response mode may be more interesting than it first appears.

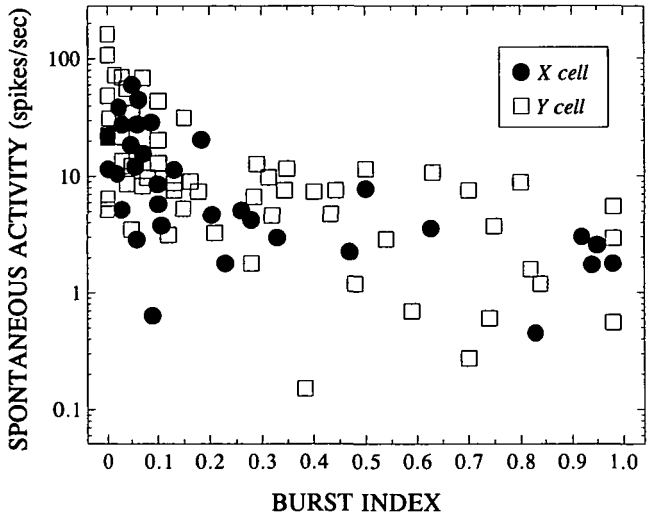

Fig. 1. Scatterplot showing the relationship between spontaneous activity and burst index. Burst index is defined as the percentage of stimulus trials evoking a low threshold burst, which is always the initial response when it occurs.

Effect of response mode on signal detection

The lower spontaneous firing of cells in burst response mode in conjunction with our earlier evidence that cells in burst mode respond vigorously to visual stimuli (Guido et al., 1992; Lu et al., 1992, 1993, see also below) together suggest that the burst mode might be associated with a higher signal-to-noise ratio than is the case for the tonic mode. This, in turn, suggests that the burst mode might be better suited to signal the presence of a stimulus. To address this possibility, we adopted the techniques of signal-detection theory and ROC analysis (Green & Swets, 1966; Macmillan & Creelman, 1991) as applied to responses of single neurons (Cohn et al., 1975; Tolhurst et al., 1983; Wilson et al., 1988; Holdefer et al., 1989; Britten et al., 1992).

Examples from intracellular recording

A powerful means to determine the role of response mode in signal detection is to study this during tonic and burst mode firing for the same cell. This can most directly be accomplished during intracellular recording by altering membrane potential *via* current injection to inactivate or de-inactivate the low threshold conductance in a controlled manner (Lo et al., 1991; Lu et al., 1992, 1993). It is then possible to apply ROC analysis to the cell's spontaneous and visually driven activity during each response mode. Unfortunately, the extreme difficulty of maintaining intracellular recording of sufficient quality and time *in vivo* precluded such a detailed analysis of a large population of cells, and we thus resorted to a less direct means of analysis based on extracellular recording. Nonetheless, consistent results from the 13 intracellular recordings serve to introduce and exemplify the effects of response mode on signal detection, and these results are described in Figs. 2 and 3 for a typical one of these cells.

Fig. 2 shows visually driven and spontaneous activity of a geniculate X cell at two different membrane potentials. The visu-

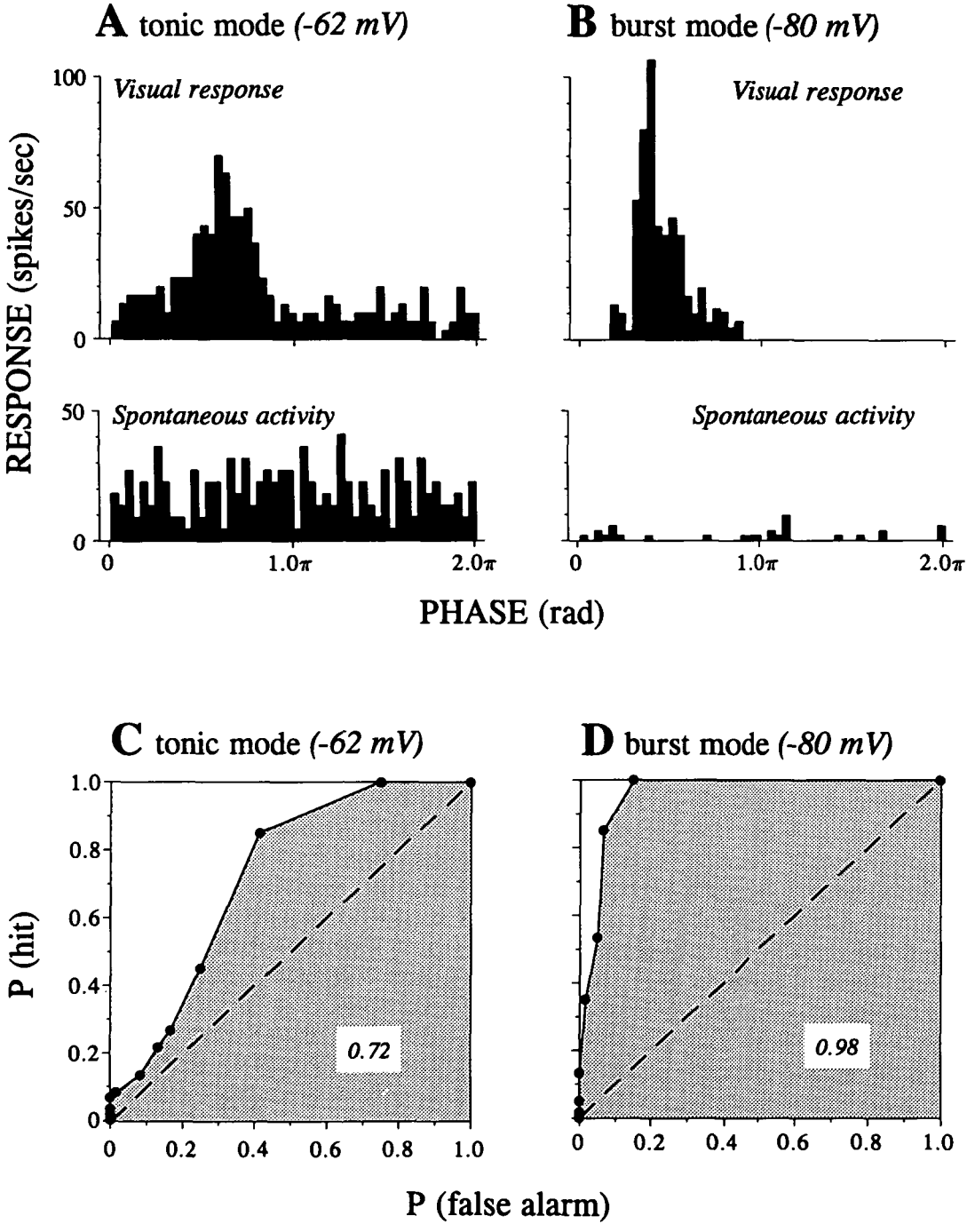

Fig. 2. Responses and ROC curves to one cycle of a drifting grating for a geniculate X cell recorded at two different membrane potentials. A: Visually driven and spontaneous activity at −62 mV. The low threshold spike was inactivated at this membrane potential and thus none were seen, leading to a purely tonic response. At this membrane potential, the burst index was 0 (see Methods). The spontaneous activity is relatively high. B: Visually driven and spontaneous activity at −80 mV. The low threshold spike was de-inactivated at this membrane potential, and EPSPs evoked by visual stimulation readily activated it. Thus, most of the action potentials rode the crests of low threshold spikes, and the cell responded primarily in burst mode. At this membrane potential, the burst index was 0.75. The spontaneous activity is relatively low, presumably because spontaneous EPSPs cannot readily activate low threshold spikes (see Discussion). C: ROC curve based on the responses in A. ROC curves for these data were based on spike counts within τ_n and τ_s for 80 trials of activity. The ROC curve plots the probability of correctly detecting visually driven from spontaneous activity. The probability of detecting the signal, *P (hits)*, is plotted on the ordinate against the probability of mistaking spontaneous activity for visually driven activity *P (false alarms)* at all possible criterion levels. The area under each curve is stippled. A curve tracing the left and top boundaries of the unit square would encompass an area of 1, indicating perfect detection of signal from noise. A curve along the dashed line of unity slope would encompass an area of 0.5, indicating that signal and noise are indistinguishable. The ROC area is shown for each curve. The remaining ROC curves in this and remaining figures follow the same convention. D: ROC curve based on the responses in B.

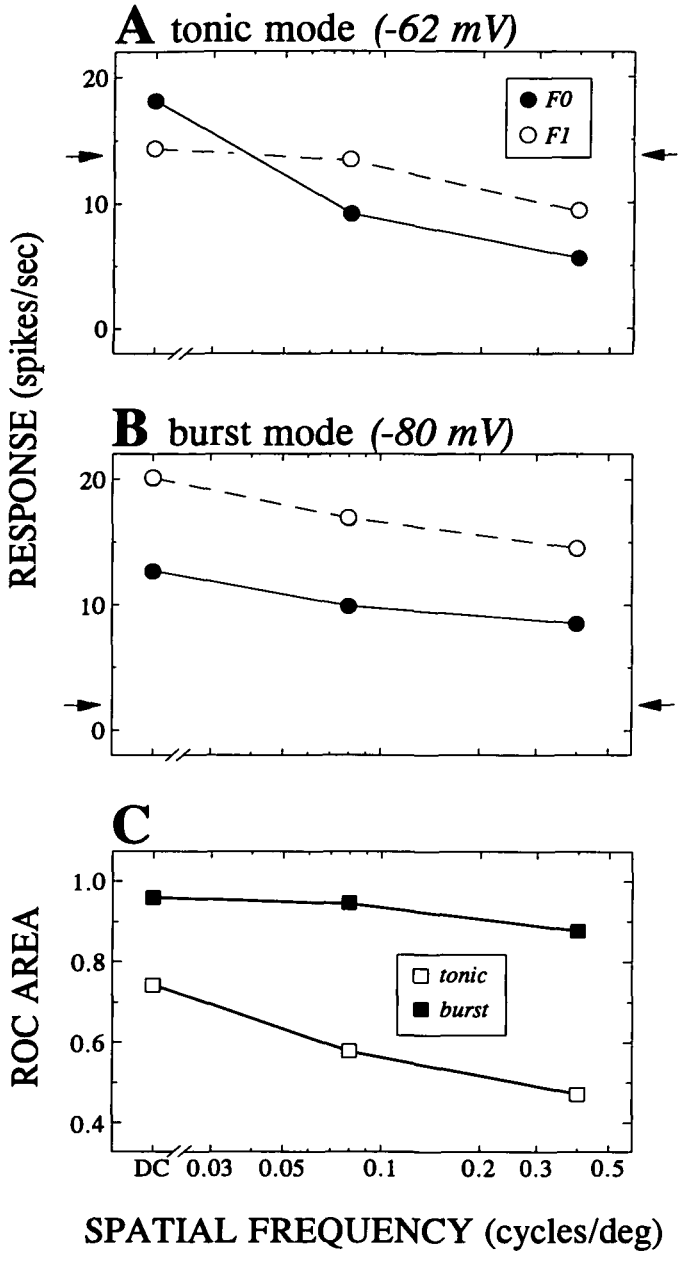

Fig. 3. Responses of a geniculate X cell to different spatial frequencies during tonic and burst firing mode; same cell as shown in Fig. 2. Both the F0 and F1 Fourier components are shown. The arrows in A and B indicate the level of spontaneous activity. A: Responses during tonic mode. B: Responses during burst mode. C: ROC area as a function of spatial frequency during both tonic and burst modes.

ally driven activity was evoked by a sine-wave grating drifted at or near spatial and temporal frequencies that elicited the maximum response, while spontaneous activity was measured during the presentation of a diffuse field of equal average luminance to the grating. For this cell, responses to zero-frequency (d.c.) modulation of the display at the optimal temporal frequency exceeded that for any higher spatial frequency, so we used d.c. stimulation for this example. When we held the neuron at the relatively depolarized level of −62 mV (Fig. 2A), the visual response was entirely of the tonic mode: we saw no evidence of low threshold bursting. This was because the underlying low threshold conductance was inactivated at this membrane potential (see Introduction; see also Jahnsen & Llinás, 1984*a*,*b*; Deschênes et al., 1984; Crunelli et al., 1989). When hyperpolarized to −80 mV (Fig. 2B), the cell switched completely from tonic to burst firing mode, and thus each cycle of the drifting grating evoked a low threshold spike and associated burst discharge. Despite the relatively robust response during the burst response mode, the relatively all-or-none nature of these responses added a substantial nonlinear distortion to the visually driven activity (Guido et al., 1992; Lu et al., 1992, 1993; and see Discussion). Note also that clear reduction in spontaneous activity when the response shifted from tonic to burst mode (Figs. 2A and 2B).

We constructed ROC curves from the intracellular responses recorded at these two membrane potentials, and these are shown in Figs. 2C and 2D. As can be seen, the ROC area was substantially larger during burst response mode (ROC area of 0.98; Fig. 2D) than during tonic response mode (ROC area of 0.72; Fig. 2C). Note that, while the ROC area is monotonically related to signal detectability, this relationship is nonparametric and nonlinear (Pollack & Hsieh, 1969; Macmillan & Creelman, 1991), and small differences between larger ROC areas (i.e. approaching 1.0) actually reflect larger differences in detectability (see below).

As noted, Fig. 2 reflects signal detection for visual targets of optimal spatial and temporal frequencies. Fig. 3 shows that this improvement of signal detection relative to the tonic mode actually increases somewhat for nonoptimal stimuli. Here, spatial frequencies other than d.c. are used as nonoptimal stimuli. Figs. 3A and 3B show limited spatial tuning curves during tonic and burst response modes. Both the fundamental Fourier response component (F1) and overall response (F0) to the drifting grating are shown; the spontaneous activity is indicated by the arrows on the left and right ordinate. Four features are worth noting about these responses. First, for a given response mode, responses to nonoptimal spatial frequencies were weaker, but spontaneous activity, by definition, remained constant. Second, spontaneous activity was substantially lower at the hyperpolarized level of −80 mV. Third, the tuning curves were similar, both in shape and amplitude, for the two response modes. Fourth, the ROC areas were smaller for all spatial frequencies during the tonic mode than during the burst mode. When these ROC areas were plotted as a function of spatial frequency in Fig. 3C, different effects were seen as the visual stimulus became less optimal. During tonic mode (open squares), the ROC areas decreased more dramatically as the spatial frequency departed from optimal and actually passed below 0.5 at a spatial frequency of 0.4 cycles/deg. During the burst mode (filled squares), however, the ROC areas changed somewhat less with spatial frequency. The flatter relationship during burst mode is related to its nearly all-or-nothing pattern of response (see Discussion). While the burst mode compared to the tonic mode offers a substantial improvement in detectability for salient stimuli (e.g. for the d.c. stimulus), only the burst mode provides reliable signal detection for the 0.4 cycles/deg stimulus. The advantage of burst firing for signal detection thus actually improved for less salient targets.

Analysis of responses recorded extracellularly

With our current techniques, intracellular recording *in vivo* is an impractical means of obtaining a large cell sample for

which detailed stimulus/response measures can be obtained. We thus applied signal detection and ROC analysis to a much larger sample of responses obtained through extracellular recording and used the data obtained from the limited cell sample *via* intracellular recording as a guide to study extracellular responses. As mentioned above, we could readily distinguish between tonic and burst response modes during extracellular recording (Guido et al., 1992; Lu et al., 1992, 1993).

Responses to gratings having optimal stimulus parameters. Initially, we performed an ROC analysis on the responses of 43 neurons to sine-wave gratings drifted at or near optimal values of spatial and temporal frequency (typically 0.1–1 cycles/deg and 4 Hz) at a contrast of 0.5. Fig. 4 shows typical examples of ROC curves with ROC areas for geniculate cells generated in response to such gratings. Shown is one example each for an X and Y cell with low burst indices (Figs. 4A and 4B) and an X and Y cell with high burst indices (Figs. 4C and 4D). Even when tested with gratings that evoked maximum activity, neurons responding more often in burst mode tended to exhibit larger ROC areas. Fig. 5A shows the relationship between ROC and burst index for our population of cells responding to optimal gratings. These values are significantly and positively correlated (for all cells, $r_s = +0.54$, $P < 0.001$; for X cells, $r_s = +0.77$, $P < 0.001$; and for Y cells, $r_s = +0.45$, $P < 0.01$).

Since ROC area can be influenced by a change in visual stimulation (signal) and/or spontaneous activity (noise), we looked at the effects of response mode separately on each of these variables. Fig. 5B shows the relationship between burst index and spontaneous activity for these cells, and Fig. 5C shows the relationship for visually driven activity. These values for spontaneous and visually driven activity were based on τ_s and τ_n, respectively, as described in Methods. As expected from Fig. 1, spontaneous activity was significantly and negatively correlated with burst index (for all cells, $r_s = -0.60$, $P < 0.001$; for X cells, $r_s = -0.78$, $P < 0.001$; and for Y cells, $r_s = -0.47$, $P < 0.01$). Visually driven activity was much less affected by response mode, and no clear correlation was seen with burst index (for

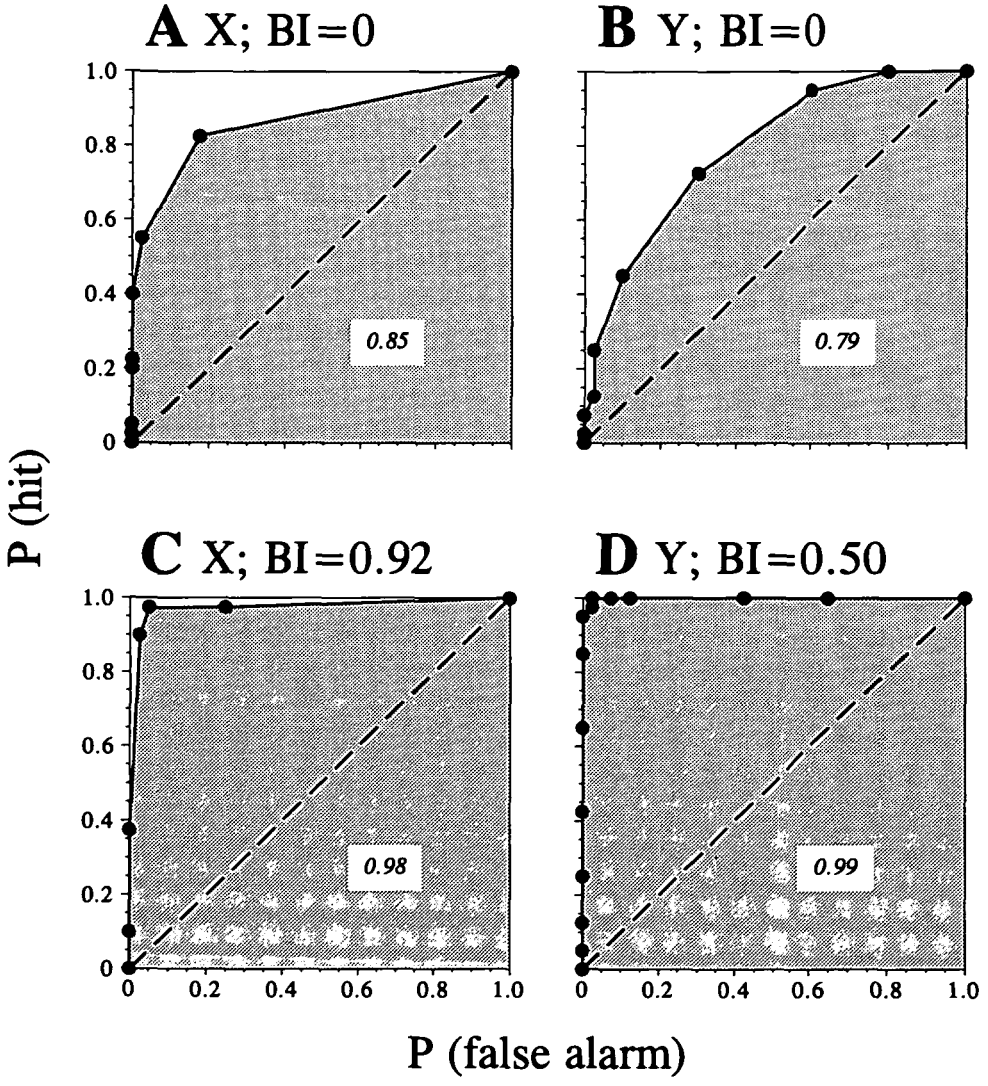

Fig. 4. ROC curves for four representative geniculate neurons. The examples are based on extracellularly recorded responses to gratings drifted at or near optimal values of spatial and temporal frequency. The burst index (*BI*) and ROC area (in the white box) is indicated for each cell.

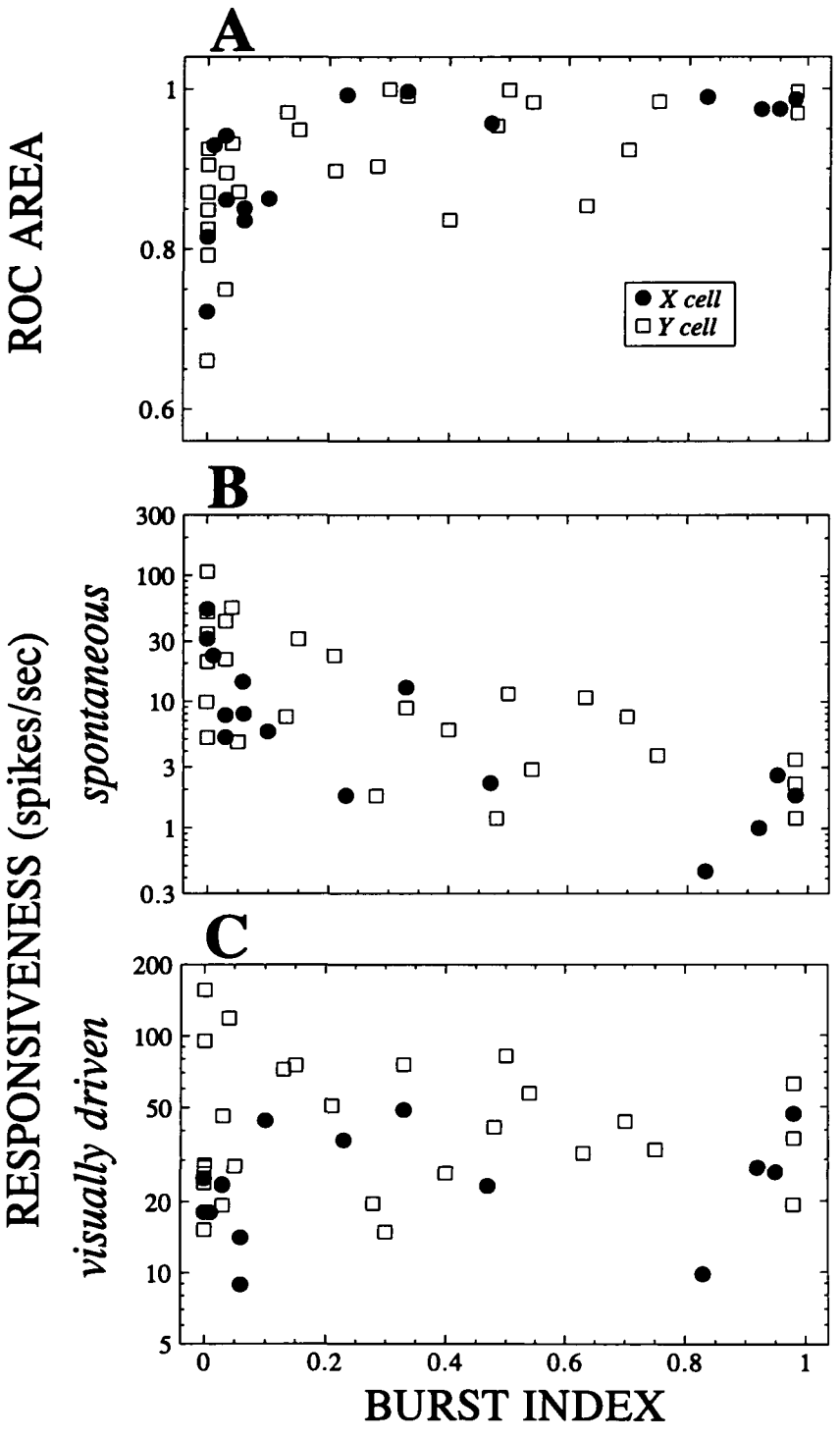

Fig. 5. Scatterplots of burst index *vs.* ROC area and response measurements for geniculate cells responding to gratings drifted at or near optimal values for spatial and temporal frequency. A: Burst index *vs.* ROC area. B: Burst index *vs.* spontaneous activity. C: Burst index *vs.* visually driven activity.

all cells, $r_s = +0.16$, $P > 0.1$; for X cells, $r_s = +0.29$, $P > 0.1$; and for Y cells, $r_s = +0.07$, $P > 0.1$). If anything, visually evoked responses were slightly higher as the cells fired more often in burst mode, but this trend was not statistically significant. It is this combination of little change in mean visually driven activity and decreasing spontaneous activity as cells respond more frequently in burst mode that endows these cells with larger ROC areas, and thus better signal detection.

Responses to gratings having nonoptimal stimulus parameters. The above analysis was performed for responses to gratings of high contrast and spatiotemporal parameters designed to evoke the maximum response. Such responses provided the largest areas for ROC curves. That is, they provide estimates of peak detectability. If, as we have shown, the burst response mode affords greater signal detectability than does the tonic mode, then this might become more important for less salient

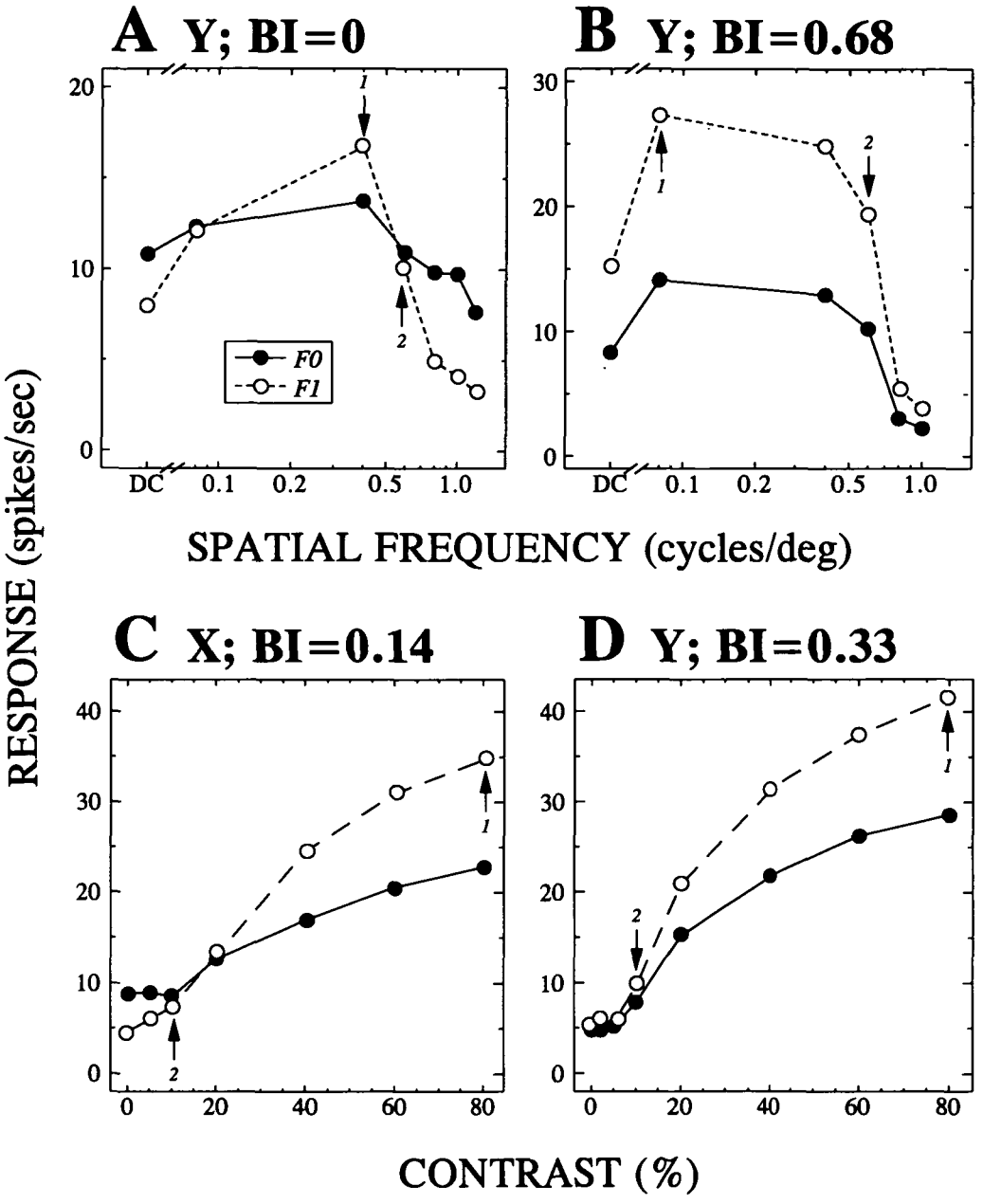

Fig. 6. Spatial tuning and response *vs.* contrast functions for four representative geniculate neurons. Both the F0 and F1 Fourier response components are indicated. The numbered arrows indicate responses used for ROC analysis: arrows labeled as 1 refer to responses at optimal spatial frequency or high stimulus contrast; arrows labeled as 2 refer to responses at nonoptimal spatial frequency or low stimulus contrast. Burst index (*BI*) is also shown for each cell. A: Spatial tuning function for an X cell responding in tonic mode. B: Spatial tuning function of a Y cell responding in burst mode. C: Contrast-response function of an X cell responding in tonic mode. D: Contrast-response function of a Y cell responding in burst mode. It should be noted here that the nearly all or none nature of the low threshold spike would lead to the prediction of an abrupt or step-like increase of response with contrast for a bursting cell. This is not so evident in E, because this cell, with a burst index of 0.33, has enough tonic responses to obscure such a relationship.

targets that are inherently more of a challenge to detect. This was suggested by our limited sample of intracellularly recorded cells (see Fig. 3C). We investigated this issue further by reducing stimulus saliency in two different ways: first, for 32 cells, we varied spatial frequency and compared ROC curves for responses to optimal *vs.* nonoptimal frequencies; second, for 27 other cells, we constructed contrast response functions and compared ROC curves for responses to low *vs.* high contrast. Two examples of each are shown in Figs. 6 and 7. Fig. 6 shows how responses for these examples vary with spatial frequency or contrast, and Fig. 7 shows how ROC area changes monotonically with contrast for a representative cell sample. Fig. 7

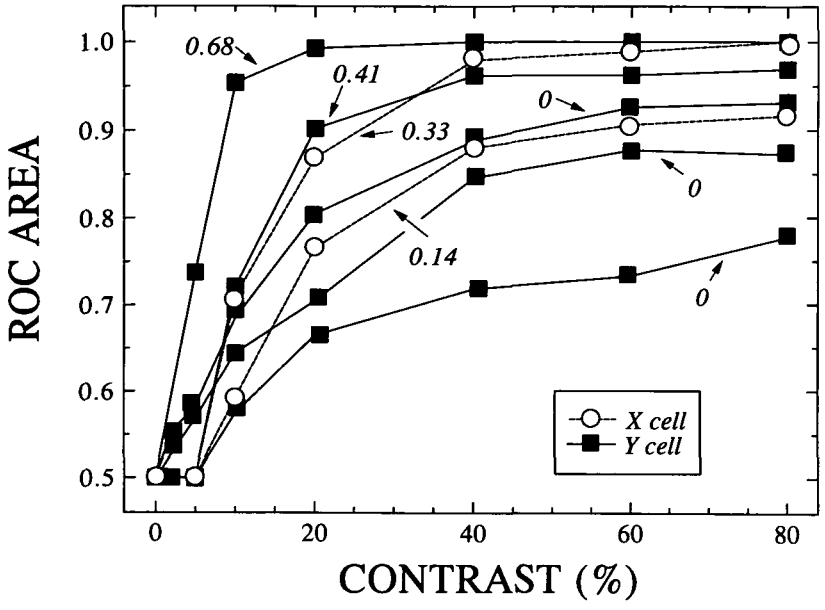

Fig. 7. Effects of grating contrast on ROC area for representative cells; burst indices are shown for each curve.

illustrates an important feature of our data: the burst response mode, when it imparts an advantage in signal detectability for one contrast level (as it almost always does), imparts such an advantage for all contrasts evoking reliable responses.

To study this issue systematically for our entire cell population, we constructed two ROC curves for each geniculate cell: one based on responses to gratings at an optimal spatial frequency or highest contrast level below saturation (see Fig. 6, arrows numbered as *1*), and the other based on responses to gratings of nonoptimal spatial frequency or lower contrast (see Fig. 6, arrows numbered as *2*). To compare these analyses of varying spatial frequency and contrast across our population of cells, we chose less salient stimuli to which the responses were roughly 1 standard deviation above spontaneous activity and >2 standard deviations lower than the peak activity. Burst index did not vary appreciably or in any consistent manner among cells when we used the different stimuli, but to be consistent, we used a single burst index for each cell, which was that based on its response to the optimal stimulus. Fig. 8 shows the results of this analysis for our population of cells, which includes 22 X and 37 Y cells. We have plotted ROC area *vs.* burst index for optimal stimulus parameters (Fig. 8A) and for nonoptimal stimulus parameters (Fig. 8B). The reduction in ROC area in response to a nonoptimal stimulus was similar whether due to a nonoptimal spatial frequency or a contrast lower than 0.5, and thus we pooled these nonoptimal conditions in Fig. 8B. As expected, we found ROC areas for responses to nonoptimal stimuli to be less than those for optimal stimuli (on binomial tests, $P < 0.001$ for all cells and either subpopulation of X or Y cells), and for this population, these ROC areas were positively correlated within cells (for all cells, r_s +0.52, $P < 0.001$; for X cells, $r_s = +0.48$, $P < 0.01$; and for Y cells, $r_s = +0.56$, $P < 0.001$). We also found interesting relationships between burst index and ROC area: although a significant positive correlation was generally found for both optimal stimuli (Fig. 8A; for all cells, $r_s = +0.36$, $P < 0.01$; for X cells, $r_s = +0.72$, $P < 0.001$; but for Y cells, $r_s = +0.24$, $P > 0.1$) and nonoptimal stimuli (Fig. 8B; for all cells, $r_s = +0.72$, $P < 0.001$; for X cells, $r_s = +0.73$, $P < 0.001$; and for Y cells, $r_s = +0.67$, $P < 0.001$), the correlation was stronger for nonoptimal stimuli, especially for Y cells.

Fig. 8C plots for each cell the relationship between burst index and the detectability ratio. The detectability ratio in this case was the ROC area for the optimal stimulus divided by that for the nonoptimal stimulus. Fig. 8C shows a significant correlation between this ratio and burst index (for all cells, $r_s = +0.71$; $P < 0.001$; for X cells, $r_s = +0.62$, $P < 0.01$; and for Y cells, $r_s = +0.69$, $P > 0.01$), indicating that the more often the cell responded in burst mode, the less its detection dropped off for less salient stimuli. This suggests that burst activity became even more important for detecting nonoptimal stimuli.

Responses to centered spots of light. In addition to ROC measures of responses to sine-wave gratings, we performed analogous measures of responses to flashing bright or dark spots for 42 additional cells. Examples for four of these cells are shown in Fig. 9. The examples in Fig. 9 are typical: cells more often in burst mode had larger ROC areas than did those more often in tonic mode. Fig. 10, which plots for each cell the relationship between burst index and ROC area, illustrates this for the population of cells tested with spots. Overall, these data were consistent with those based on responses to gratings: there was a positive correlation between burst index and ROC area (for all cells, $r_s = +0.51$, $P < 0.001$; for X cells, $r_s = +0.68$, $P < 0.001$; for Y cells, $r_s = +0.41$, $P < 0.01$).

We noted that 14% of the cells (13/90) responded exclusively in tonic mode and that 86% of the cells (77/90) responded on at least some trials in burst mode (i.e. they had a burst index >0 and <1). For this latter group, this means that the response mode varied among individual response trials during the average process. We controlled for this variability in a subset of 22 cells that switched between tonic and burst mode during recording. For these, we recorded at least 100 trials of visually driven and spontaneous activity, and sorted activity on a trial-by-trial basis into tonic and burst components. To ensure enough trials representing each response mode, we selected only the subset of cells with burst indices between 0.10 and 0.90, which is why the subset was limited. Once we sorted the response trials,

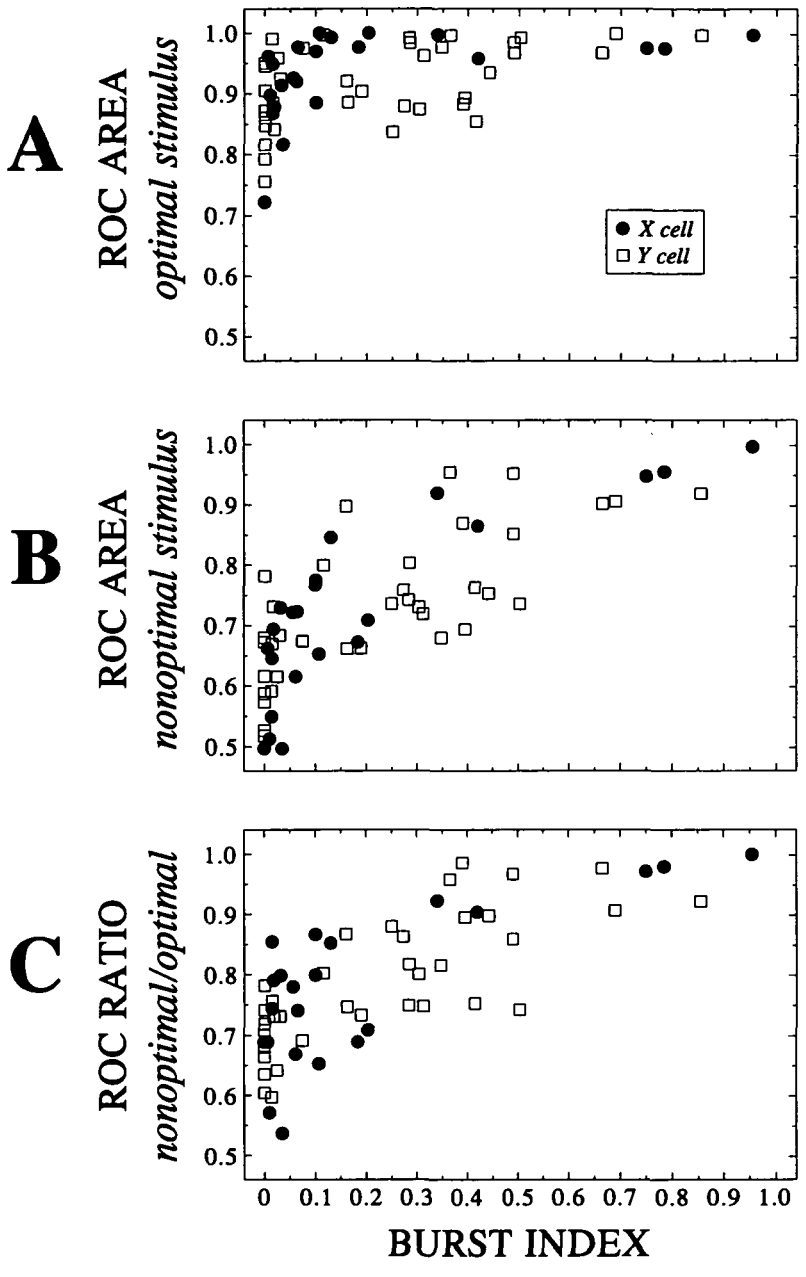

Fig. 8. Relationship between burst index and ROC area for responses to drifting gratings. A: Burst index *vs.* ROC area for responses to optimal spatial frequency or high stimulus contrast. B: Burst index *vs.* ROC area for responses to nonoptimal spatial frequency or low stimulus contrast. C: Burst index *vs.* ratio of ROC areas for responses to nonoptimal and optimal stimuli. The ratio for each cell is the ROC area for the nonoptimal stimulus over that for the optimal stimulus.

we generated two ROC curves for each cell, one based on its tonic response, the other on its burst response. Figs. 11–13 show ROC curves for three representative geniculate cells analyzed in this fashion. In every case, the ROC area was larger for the burst responses than for the tonic responses. This was true for both X (Fig. 11) and Y cells (Figs. 12 and 13) and also for responses to spots of both high contrast (Figs. 11 and 13) and low contrast (Fig. 12).

The results of our within-cell analysis are summarized in Fig. 14. For each cell, we plotted ROC area for its burst component against that for its tonic component. We have further divided the data on the basis of spot contrast: 11 cells were tested with a high-contrast spot (Fig. 14A; analogous to optimal grating stimuli represented in Fig. 8A); 15 were tested with a low-contrast spot (Fig. 14B; analogous to nonoptimal grating stimuli represented in Fig. 8B); and thus four cells were tested at both spot contrasts. Note that every cell had a larger ROC area during its burst response mode than during its tonic mode, because every point lay above the line of unity slope in Figs. 14A and 14B. These differences were significant for response both to high- and low-contrast spots ($P < 0.001$ on a binomial test for each spot contrast). The bar graphs in Figs. 14C and 14D further illustrate the differences between tonic and burst modes. For responses to high-contrast spots (Fig. 14C), visually driven activity was greater and spontaneous activity was less during the burst mode than during the tonic mode ($P < 0.02$ and $P < 0.01$, respectively, on binomial tests). The same relationships held during response to the low-contrast spots (Fig. 14D; $P < 0.001$ on binomial tests for both comparisons).

In parallel with the analysis represented by Fig. 8C, we sought to determine whether the improvement in signal detection associated with the burst response mode was relatively greater for

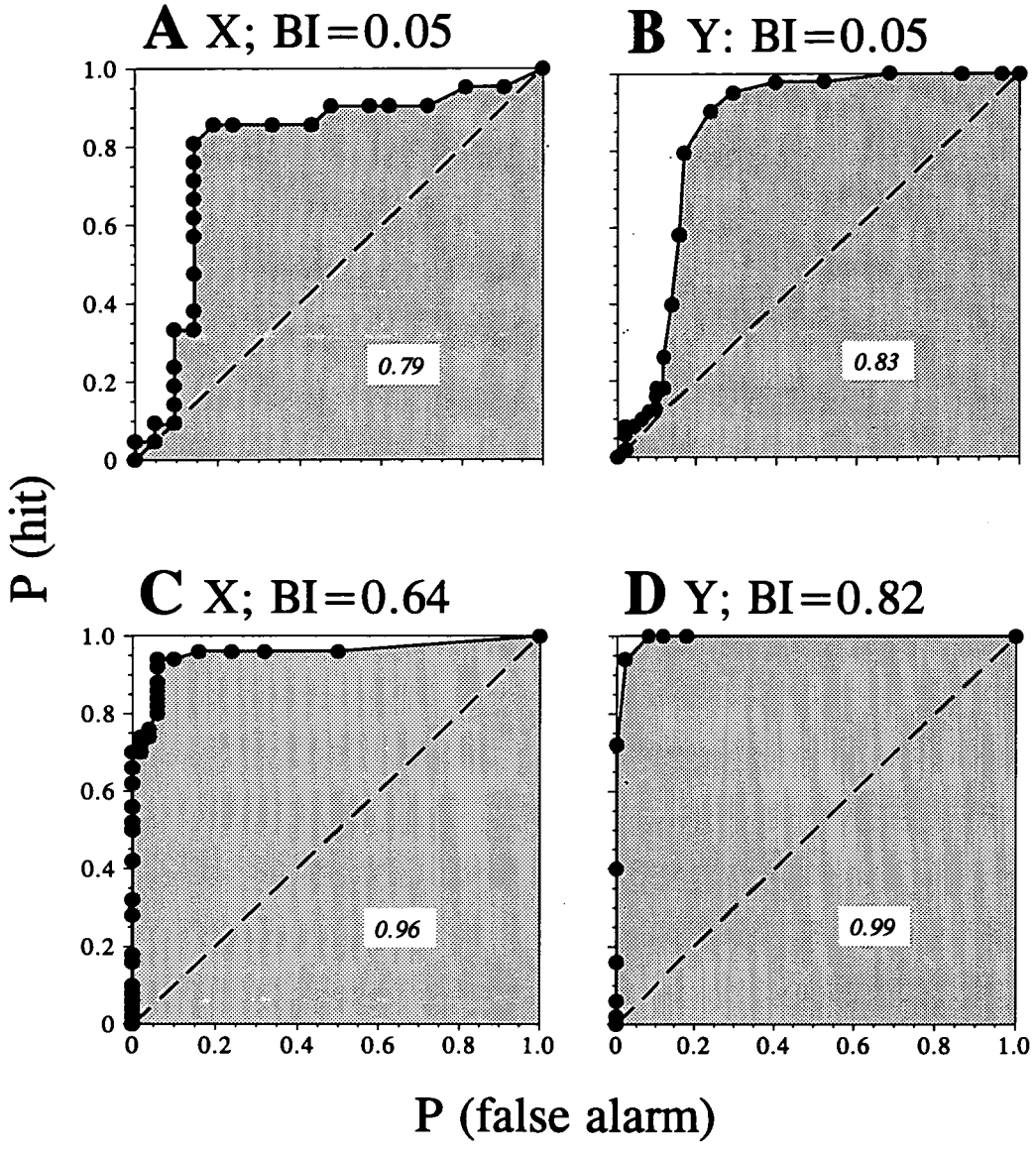

Fig. 9. ROC curves for four representative geniculate neurons; conventions are as in Fig. 4. The examples are based on extracellularly recorded responses to spots flashed on the cell's receptive-field center.

responses to lower contrast stimuli. To address this, we computed a ratio of ROC areas for each cell. This ratio was equal to the ROC area associated with a cell's tonic response over that associated with its burst response (i.e. the ordinate-to-abscissa ratio for each point plotted in Figs. 14A and 14B). Fig. 14E shows the mean and standard error for these ratios, which, as expected, are both less than 1. Note, however, that these ratios were significantly lower for cells tested with low-contrast spots than for those with high-contrast spots ($P < 0.001$, on a Mann-Whitney U test). Thus, compared to tonic mode, burst mode improved detectability more for low-contrast spots than for high-contrast ones, and it supported the results of the analogous study of responses to gratings (Fig. 8C).

While ROC area provides an index of detectability, the index is nonparametric and nonlinear. In particular, small differences between relatively large ROC area represent large detectability differences (Macmillan & Creelman, 1991). Under appropriate conditions (i.e. among other things, knowledge that the distributions for *hits* and *false alarms* are normally distributed), ROC data can be normalized to d' values, permitting a more linear and parametric comparison of detectability (Green & Swets, 1966; Pollack & Hseih, 1969; Macmillan & Creelman, 1991). Since not all of the data from our cells met the criteria for conversion of ROC data to d' values, we did not formally do this and thus present our data nonparametrically. However, while such a conversion is not justified for formal comparisons, it may nonetheless be useful as a rough guide to detectability differences. When such a conversion is done for the cells illustrated in Fig. 14, the result is that, on average, burst mode provides better detectability than tonic mode for high-contrast stimuli by a factor of 1.7, and for low-contrast stimuli the detectability improvement is by a factor of 4.5. These numbers probably

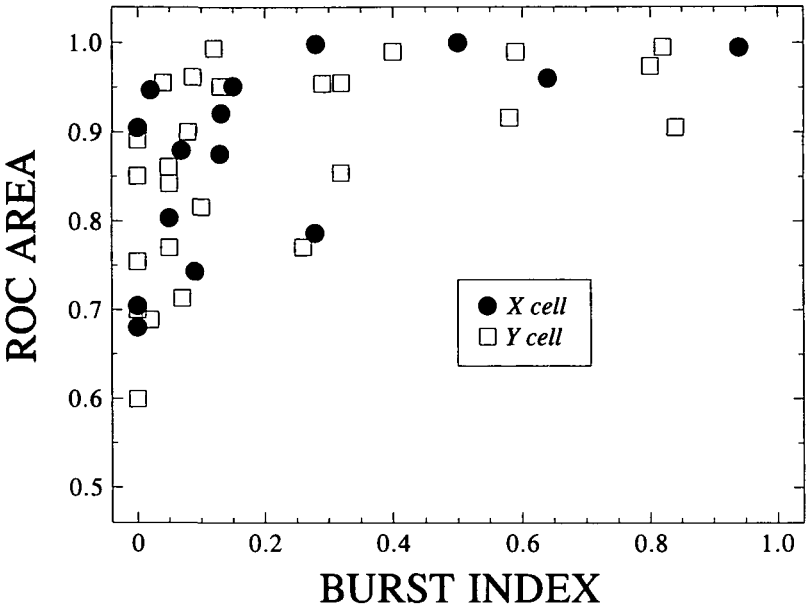

Fig. 10. Relationship between burst index and ROC area for responses to flashing spots; conventions are as in Figs. 8A and 8B.

provide a rough approximation of the detectability differences between burst and tonic mode under the conditions of visual stimulation described.

Discussion

We used ROC analysis to assess how effectively geniculate cells *detect* visual targets while responding in tonic or burst modes. We generated ROC curves from neuronal responses of geniculate cells and used the area under each curve as an index of detectability (Green & Swets, 1966; Pollack & Hsieh, 1969; Macmillan & Creelman, 1991). This analysis indicates that burst responses better support signal detection than do tonic responses. The more cells responded to visual stimuli in burst mode, the larger their ROC areas, and for individual cells, their ROC areas were larger during burst mode than during tonic mode. Our analysis also showed that the advantage in detectability brought about by burst firing was greater during responses to less optimal visual stimuli. These features applied to both X and Y cells, with no obvious difference between types.

Differences in responses during burst and tonic firing

Signal-to-noise ratios

A cell's ability to signal the presence of a visual stimulus is determined by the level of visually driven activity relative to spontaneous activity, or the signal-to-noise ratio (Barlow & Levick, 1966; Tolhurst et al., 1983; Wilson et al., 1988). One might predict that burst firing would promote lower levels of response during *both* spontaneous activity and visually evoked discharges due to the silent periods before each low threshold Ca^{2+} spike, although the burst of action potentials itself would somewhat counteract this. Nonetheless, we found in the present study that both burst and tonic firing modes provided roughly equal amplitudes of visually driven discharge, but that burst firing was associated with a reduced level of spontaneous activity. Thus, the signal-to-noise ratio was much greater during burst mode than during tonic mode, and this is the major reason for the greater signal detectability associated with burst firing. These different signal-to-noise ratios for burst and tonic firing are consistent with the underlying differences between these two response modes (see Introduction).

During burst mode, the cell responds initially from a relatively hyperpolarized level, which is necessary to de-inactivate the low threshold spike. From this level, a sufficiently large depolarization or EPSP will activate the low threshold spike, which is a large, relatively all-or-none depolarization usually sufficient to evoke a burst of action potentials. In other words, the low threshold spike can be viewed as an amplification step that permits a hyperpolarized cell to respond robustly to a sufficiently large depolarization, such as may be evoked by a visual stimulus. Because of its relative all-or-none nature, this amplification is highly nonlinear (see below). Thus, the basis for the strong visual response or signal during burst response mode is the amplification afforded by the low threshold spike. If so, then why is the spontaneous activity so much lower during burst mode than during tonic mode, a phenomenon we have invariably noted (Lo et al., 1991; Lu et al., 1992, 1993)? EPSPs that are too small will not activate the low threshold spike, just as subthreshold EPSPs cannot activate conventional action potentials during tonic mode. Also, even though the low threshold spike is nearly all or none, it is not completely so, and thus smaller EPSPs may evoke a small low threshold spike that is not large enough to evoke action potentials. We have commonly observed during intracellular recording that summated EPSPs evoked by salient visual stimuli are consistently much larger than spontaneous EPSPs (Lo et al., 1991; Lu et al., 1992, 1993). We thus conclude that spontaneous EPSPs commonly are too small to fully activate low threshold spikes during burst mode, but such EPSPs are large enough to increase spontaneous activity during tonic mode. This would happen if, for instance, the threshold for de-inactivation of the low threshold spike were sufficiently far below its full activation threshold that an EPSP

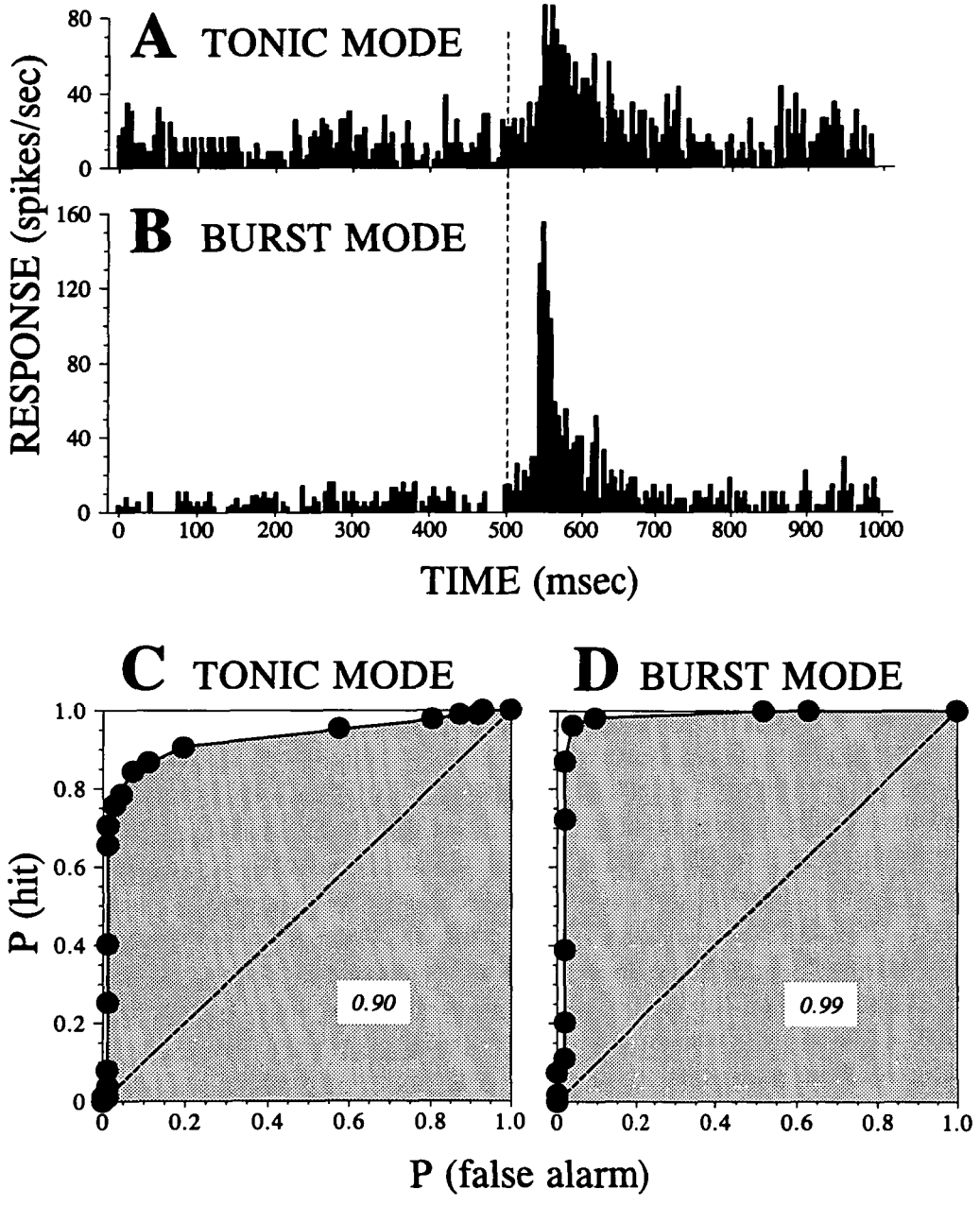

Fig. 11. Responses and ROC curves for a geniculate X cell to a flashing spot of high stimulus contrast. Responses were sorted into burst and tonic mode on a trial-by-trial basis. Separate histograms are depicted for each response mode. Stimulus onset is indicated by the vertical dashed line running through the response histograms. A: Histogram based on trials during which the cell responded in tonic mode. B: Histogram based on trials during which the cell responded in burst mode. C: ROC curve constructed from tonic responses. D: ROC curve constructed from burst responses.

might have to be much larger to reach threshold for activation of a low threshold spike than for activation of an action potential.

Linearity of response

As we have previously demonstrated, another difference exists between burst and tonic firing. Burst firing leads to more nonlinear distortion in the response than does firing (Guido et al., 1992; Lu et al., 1992, 1993). There are at least two reasons for this.

First, as noted above, burst firing involves activation of the low threshold spike, which is a relatively all-or-none depolarization with a threshold (Jahnsen & Llinás, 1984*a*,*b*; Deschênes et al., 1984; Steriade & Llinás, 1988; Crunelli et al., 1989). In this regard, it resembles the conventional action potential. These properties mean that the relationship between the visual stimulus and the evoked firing of the cell exhibits a very limited dynamic range. Too weak a stimulus evokes too small an EPSP, causing little or no firing. As soon as the visual stimulus is large enough to evoke a suprathreshold EPSP, firing quickly attains its maximum level, with very little change for large changes in stimulus amplitude above threshold. Tonic firing has a much larger dynamic range. This is because stronger stimuli evoke

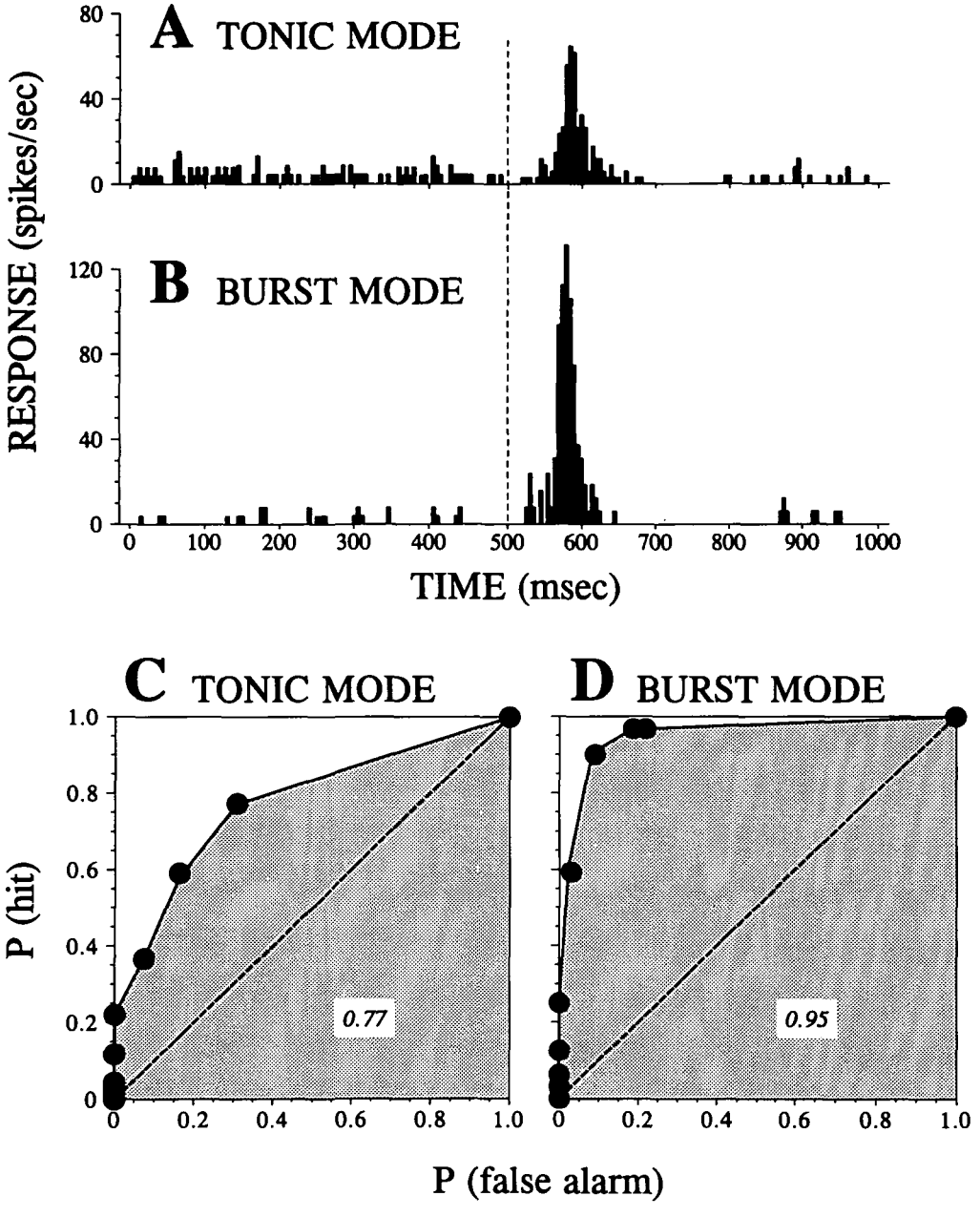

Fig. 12. Responses and ROC curves for a geniculate Y cell to a flashing spot of low stimulus contrast; conventions are as in Fig. 11.

larger EPSPs, which, in turn, lead to higher firing frequencies. The end result is that stimulus strength is more linearly coded by the firing level during tonic mode than during burst mode.

Another difference between burst and tonic firing contributes to this difference in linear summation. As noted above, tonic firing is associated with much higher levels of spontaneous activity. This higher activity permits the linear signalling of inhibitory stimuli, which would reduce firing below spontaneous levels. Obviously, firing levels can never drop below zero, and with the low spontaneous activity seen during burst firing, there is little opportunity to signal inhibition. In other words, the lower spontaneous activity during burst firing enhances half-wave rectification in the response more than is seen during tonic firing, and this rectification contributes to the greater nonlinear distortion seen during burst firing.

Effect of stimulus strength on detectability

As noted in Results, the advantage of burst firing over tonic firing as applied to signal detectability was greater for less salient stimuli. Since spontaneous activity, by definition, is not affected by changes in visual stimuli, any change seen in the detectability or ROC area must reflect changes in response levels to visual stimuli. The fact that stimulus strength has less influence on the ROC area during burst firing can be explained by the more limited dynamic range of this response mode. During burst mode, any visual stimulus sufficiently strong to evoke low

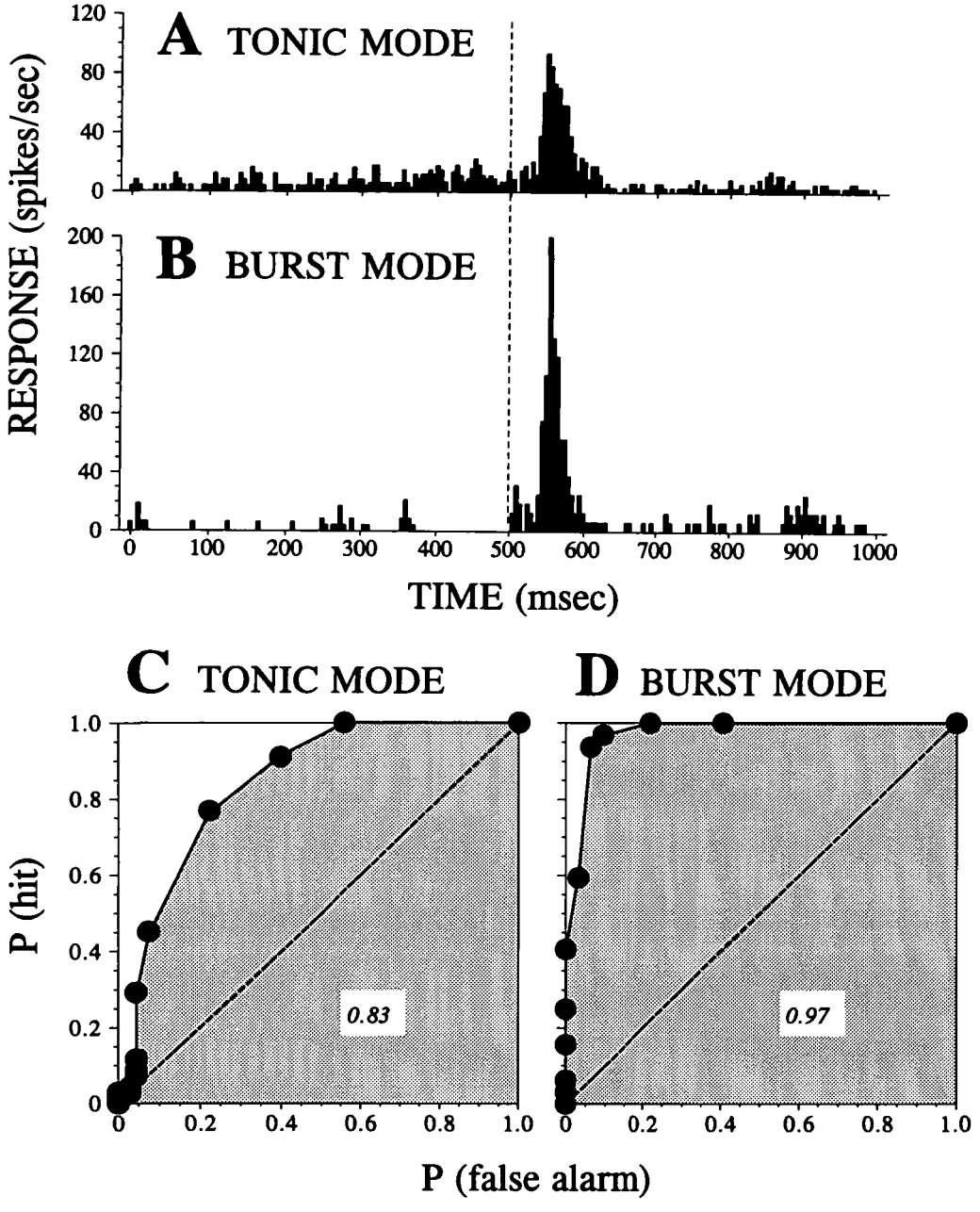

Fig. 13. Response and ROC curves for a geniculate Y cell to a flashing spot of high stimulus contrast; conventions are as in Fig. 11.

threshold spiking will evoke a near-maximum firing rate, and increasing stimulus strength within the suprathreshold range will have little further effect on the low threshold spike or evoked action potentials. Put another way, the firing level evoked by a strong stimulus (i.e. at optimal spatial frequency or high contrast) will be reduced rather little as the stimulus becomes weaker, as long as the stimulus remains above threshold. Thus, the ROC area changes relatively little for changes in stimulus strength for suprathreshold stimuli. In contrast, the greater dynamic range during tonic firing results in a greater reduction of firing level for weaker stimuli, and this results in a larger dependence of detectability on signal strength.

Hypothesis for burst and tonic firing

Our data indicate that geniculate relay cells transmit very different signals to visual cortex during burst and tonic firing. During burst firing, the cell responses have a higher ROC area, meaning that the relay cell is better able to signal the presence of a visual stimulus. As noted above, this greater signal-to-noise ratio is chiefly the result of lower spontaneous activity. However, this is achieved at the expense of response linearity, partly due to the nonlinear amplification of the low threshold spike and partly due to half-wave rectification resulting from the lower spontaneous activity. During tonic firing, the relay cell sums

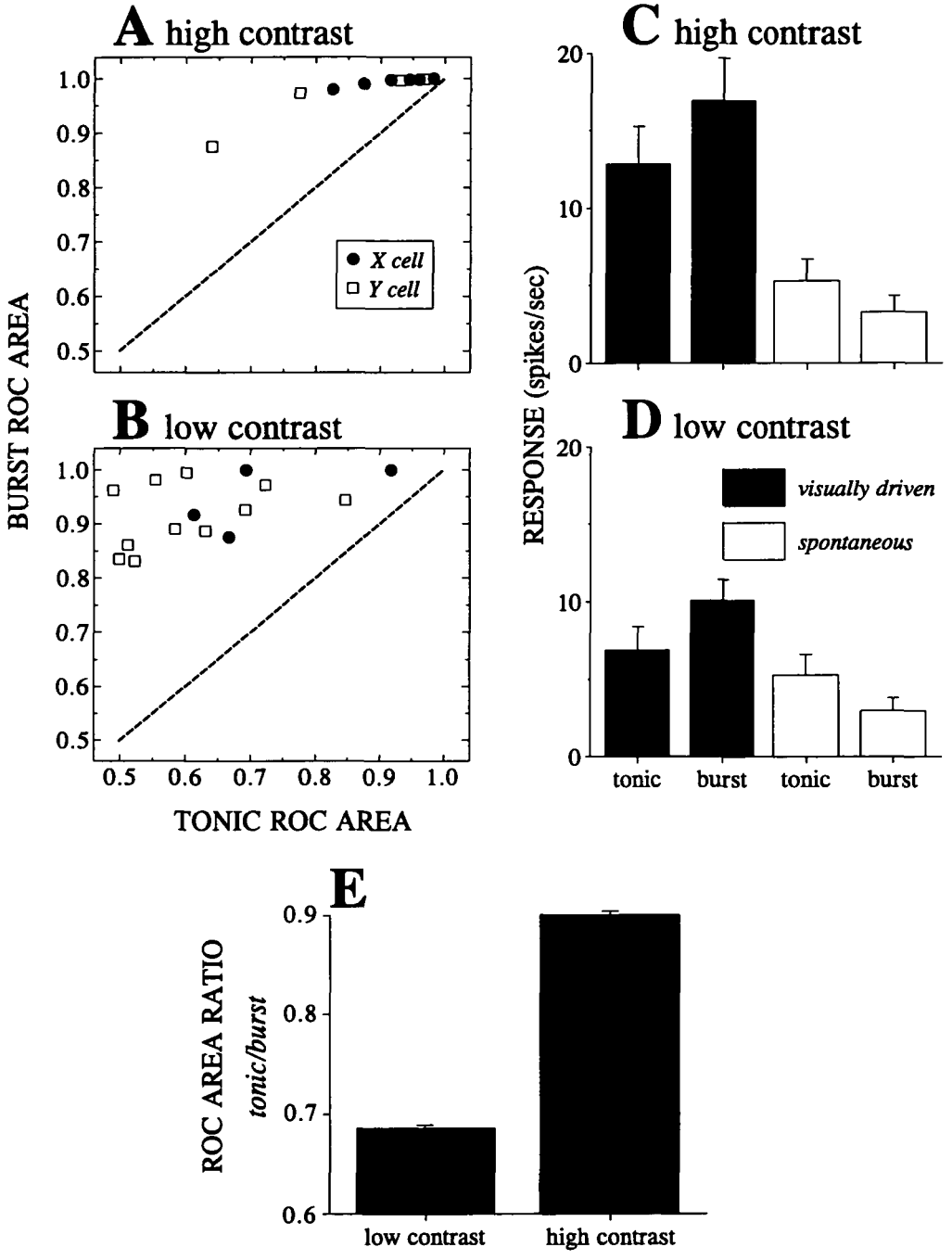

Fig. 14. Effect of response mode on detectability of flashing spot stimuli. Each of the cells shown had a burst index between 0.1 and 0.9, and all responses were sorted on a trial-by-trial basis into those occurring during tonic mode and those occurring during burst mode (i.e. as for Figs. 11–13). A: Tonic *vs.* burst ROC areas for spots of higher contrast. B: Tonic *vs.* burst ROC areas for spots of lower contrast. The dashed lines in A, B have a slope of 1, and thus each cell shows a greater ROC area during its burst mode. C: For high contrast spots, the mean and standard error for both visually driven and spontaneous activity in each response mode. D: For low contrast spots, the mean and standard error for both visually driven and spontaneous activity in each response mode. E: ROC area ratio for high and low contrast spots computed from A, B. The ratio for each cell represents the ROC area during its burst mode divided by that during its tonic mode, and the means and standard errors of these values are shown.

visual stimuli more linearly, meaning that it relays information with greater fidelity. This is partly due to the removal of a nonlinear response component (i.e. the low threshold spike) and partly due to greater levels of spontaneous activity, which reduces half-wave rectification. However, this improved linearity is achieved at the expense of signal detectability, because the requirement of a higher level of spontaneous activity serves to reduce the signal-to-noise ratio.

We suggest that these differences between burst and tonic firing may support different types of visual function. For the visual system *via* visual cortex to detect the presence of a stimulus, the signal relayed from the lateral geniculate nucleus should have a maximum ROC area. During this type of visual function, linearity of summation in the signal relayed to cortex is less important than detectability, because determining the presence of a stimulus is not compromised by nonlinear distortion of the signal. However, once a stimulus is detected and the role of the visual system changes to one of analyzing that stimulus in detail, linearity is more important. Tonic firing in relay cells better supports this function through its enhanced linear summation, and the loss in signal detectability causes little or no problem for stimuli already detected and under analysis.

This difference in function for burst and tonic firing may relate to two major forms of visual attention known as *orienting* or *scanning attention* and *focal attention* (Posner & Peterson, 1990). Scanning attention is used to detect visual stimuli and would benefit from burst firing of geniculate relay cells. Focal attention is used to analyze visual stimuli in detail and would benefit from tonic firing of geniculate relay cells. Perhaps while the visual system scans a particular part of the visual field for a potentially salient visual stimulus, the geniculate relay cells mapped to that location are kept hyperpolarized to respond in burst mode (see also Crick, 1984). If a target is located, the system may then switch these geniculate cells to relay mode so that the target can be analyzed in detail.

Our hypothesis that burst firing contributes significantly to retinogeniculate transmission during active visual behavior is very different from most prior suggestions regarding this firing mode for thalamic relay cells. A number of workers have focused on the tendency for the burst mode of firing and its underlying low threshold spike to occur rhythmically (see Steriade & Deschênes, 1984; Steriade & Llinás, 1988; Steriade et al., 1990, 1993). Such rhythmic bursting has been associated with certain states of EEG synchronization such as slow wave sleep, and they are thought to reflect this changed behavioral state. In other words, as the animal becomes drowsy or sleepy, thalamic relay cells hyperpolarize, and they begin to discharge low threshold spikes rhythmically with bursts of action potentials; this response pattern is thought to develop intrinsically to thalamus and thus be irrespective of sensory input. For the lateral geniculate nucleus, this results in a sort of functional disconnection of relay cells from their retinal inputs, and this reflects a very different role for low threshold spikes than that suggested in the present study.

It is interesting to note that cyclic bursting is seen during *in vitro* recordings, in certain *in vivo* preparations that disconnect the thalamus from its afferents, or during specific behavioral states, such as slow wave sleep (see Steriade & Deschênes, 1984; Steriade & McCarley, 1990; Steriade et al., 1990, 1993). We have observed such rhythmic bursting patterns for geniculate neurons under our experimental conditions, but only rarely (see also Guido et al., 1992; Lu et al., 1992, 1993). However, we see no reason to doubt the common presence of such activity under the proper conditions. Perhaps activity in certain afferents (e.g. retinal, cortical, or parabrachial afferents) prevents any intrinsic tendency for geniculate cells to burst rhythmically, and such rhythmic bursting becomes prominent if either the lateral geniculate nucleus is physically disconnected from these inputs (e.g. during *in vitro* recording) or if these nonretinal inputs become quiescent during certain states (e.g. slow wave sleep). The low threshold spike may thus serve a dual purpose: one during alert visual behavior, such as the support of scanning attention, and another during slow wave sleep, such as rhythmic bursting.

It is also important to note that the Ca^{2+} conductance underlying the low threshold spike is but one of many active membrane properties that geniculate neurons can express (Sherman & Koch, 1986, 1990; Steriade & Llinás, 1988; McCormick, 1992*a*,*b*). We are far from understanding how such membrane properties function and interact with each other. Nonetheless, we find that the presence or absence of low threshold spike, which corresponds to burst or tonic firing, respectively, strongly influences the pattern of action potentials relayed to visual cortex. We further suggest that these different firing patterns may be an important substrate for certain attentional phenomena. Of great interest would be to examine these response modes in an awake, behaving animal.

Acknowledgments

This research was supported by USPHS Grant EY03038. J. W. Vaughan received support from Postdoctoral Fellowship EY06340, and D. W. Godwin received support from Postdoctoral Fellowship NS09163.

References

Barlow, H.B. & Levick, W.R. (1966). Three factors limiting the reliable detection of light by retinal ganglion cells of the cat. *Journal of Physiology* (London) **200**, 1–24.

Bloomfield, S.A. & Sherman, S.M. (1988). Postsynaptic potentials recorded in neurons of the cat's lateral geniculate nucleus following electrical stimulation of the optic chiasm. *Journal of Neurophysiology* **60**, 1924–1945.

Bloomfield, S.A., Hamos, J.E. & Sherman, S.M. (1987). Passive cable properties and morphological correlates of neurones in the lateral geniculate nucleus of the cat. *Journal of Physiology* (London) **383**, 653–692.

Britten, K.H., Shadlen, M.N., Newsome, W.T. & Movshon, J.A. (1992). The analysis of visual motion: A comparison of neuronal and psychophysical performance. *Journal of Neuroscience* **12**, 4745–4765.

Cohn, T.E., Green, D.G. & Tanner, W.P. (1975). Receiver operating characteristic analysis, application to the study of quantum fluctuation effects in optic nerve of *Rana pipens*. *Journal of General Physiology* **66**, 583–616.

Crick, F. (1984). Function of the thalamic reticular complex: The searchlight hypothesis. *Proceedings of the National Academy of Sciences of the U.S.A.* **81**, 4586–4590.

Crunelli, V., Lightowler, S. & Pollard, C.E. (1989). A T-type Ca^{2+} current underlies low-threshold Ca^{2+} potentials in cells of the cat and rat lateral geniculate nucleus. *Journal of Physiology* (London) **413**, 543–561.

Deschênes, M., Paradis, M., Roy, J.P. & Steriade, M. (1984). Electrophysiology of neurons of lateral thalamic nuclei in cat: Resting properties and burst discharges. *Journal of Neurophysiology* **51**, 1196–1219.

Funke, K. & Eysel, U.T. (1992). EEG-dependent modulation of response dynamics of cat dLGN relay cells and the contribution of corticogeniculate feedback. *Brain Research* **573**, 217–227.

Green, D.M. & Swets, J.A. (1966). *Signal Detection Theory and Psychophysics*. New York: Wiley.

Guido, W., Lu, S-M. & Sherman, S.M. (1992). Relative contributions of tonic and burst response modes to the receptive field properties of lateral geniculate neurons in the cat. *Journal of Neurophysiology* **6**, 2199–2211.

Holdefer, R.N., Norton, T.T. & Godwin, D.W. (1989). Effects of bicuculline on signal detectability in lateral geniculate nucleus relay cells. *Brain Research* **488**, 341–347.

Ikeda, H. & Wright, M.J. (1975). Sensitivity of neurones in visual cortex (area 17) under different levels of anesthesia. *Experimental Brain Research* **20**, 417–484.

Jahnsen, H. & Llinás, R. (1984*a*). Electrophysiological properties of

guinea-pig thalamic neurones: An *in vitro* study. *Journal of Physiology* (London) **349**, 205–226.

JAHNSEN, H. & LLINÁS, R. (1984*b*). Ionic basis for the electro-responsiveness and oscillatory properties of guinea-pig thalamic neurones in vitro. *Journal of Physiology* (London) **349**, 227–247.

LO, F.-S., LU, S.-M. & SHERMAN, S.M. (1991). Intracellular and extracellular *in vivo* recording of different response modes for relay cells of the cat's lateral geniculate nucleus. *Experimental Brain Research* **83**, 317–328.

LU, S-M., GUIDO, W. & SHERMAN, S.M. (1992). Effects of membrane voltage on receptive field properties of lateral geniculate neurons in the cat: Contributions of the low threshold Ca^{2+} conductance. *Journal of Neurophysiology* **6**, 2185–2198.

LU, S-M., GUIDO, W. & SHERMAN, S.M. (1993). The brainstem parabrachial region controls mode of response to visual stimulation of neurons in the cat's lateral geniculate nucleus. *Visual Neuroscience* **10**, 631–642.

MACMILLAN, N.A. & CREELMAN, C.D. (1991). *Detection Theory: A User's Guide*. New York: Cambridge University Press.

MCCORMICK, D.A. (1992*a*). Cellular mechanisms underlying cholinergic and noradrenergic modulation of neuronal firing mode in the cat and guinea pig dorsal lateral geniculate nucleus. *Journal of Neuroscience* **12**, 278–289.

MCCORMICK, D.A. (1992*b*). Neurotransmitter actions in the thalamus and cerebral cortex and their role in neuromodulation of thalamocortical activity. *Progress in Neurobiology* **39**, 337–388.

POLLACK, I. & HSIEH, R. (1969). Sampling variability of the area under the ROC-curve and of d'. *Psychological Bulletin* **71**, 161–173.

POSNER, M.I. & PETERSON, S.E. (1990). The attention system of the human brain. *Annual Reviews of Neuroscience* **13**, 25–42.

SHERMAN, S.M. & KOCH, C. (1986). The control of retinogeniculate transmission in the mammalian lateral geniculate nucleus. *Experimental Brain Research* **63**, 1–20.

SHERMAN, S.M. & KOCH, C. (1990). Thalamus. In *Synaptic Organization of the Brain, 3rd edition*, ed. SHEPHERD, G.M., pp. 246–278. New York: Oxford University Press.

STERIADE, M. & DESCHÊNES, M. (1984). The thalamus as a neuronal oscillator. *Brain Research Reviews* **8**, 1–63.

STERIADE, M., JONES, E.G. & LLINÁS, R.R. (1990). *Thalamic Oscillations and Signalling*. Neuroscience Institute Publ. Series, New York: Wiley and Sons.

STERIADE, M. & LLINÁS, R.R. (1988). The functional states of the thalamus and the associated neuronal interplay. *Physiological Reviews* **68**, 649–742.

STERIADE, M. & MCCARLEY, R.W. (1990). *Brainstem Control of Wakefulness and Sleep*. New York: Plenum Press.

STERIADE, M., MCCORMICK, D.A. & SEJNOWSKI, T.J. (1993). Thalamocortical oscillations in the sleeping and aroused brain. *Science* **262**, 679–685.

TOLHURST, D.J., MOVSHON, J.A. & DEAN, A.F. (1983). The statistical reliability of signals in single neurons in cat and monkey visual cortex. *Vision Research* **23**, 775–785.

WILSON, J.R., BULLIER, J. & NORTON, T.T. (1988). Signal-to-noise comparisons for X and Y cells in the retina and lateral geniculate nucleus of the cat. *Experimental Brain Research* **70**, 399–405.